# The sacrificial adaptor protein Skp functions to remove stalled substrates from the β-barrel assembly machine

Ashton N. Combs[a] and Thomas J. Silhavy[a,1]

[a]Department of Molecular Biology, Princeton University, Princeton, NJ 08544

Edited by Joe Lutkenhaus, Department of Microbiology, Molecular Genetics and Immunology, University of Kansas Medical Center, Kansas City, KS; received August 13, 2021; accepted November 22, 2021

**The biogenesis of integral β-barrel outer membrane proteins (OMPs) in gram-negative bacteria requires transport by molecular chaperones across the aqueous periplasmic space. Owing in part to the extensive functional redundancy within the periplasmic chaperone network, specific roles for molecular chaperones in OMP quality control and assembly have remained largely elusive. Here, by deliberately perturbing the OMP assembly process through use of multiple folding-defective substrates, we have identified a role for the periplasmic chaperone Skp in ensuring efficient folding of OMPs by the β-barrel assembly machine (Bam) complex. We find that β-barrel substrates that fail to integrate into the membrane in a timely manner are removed from the Bam complex by Skp, thereby allowing for clearance of stalled Bam–OMP complexes. Following the displacement of OMPs from the assembly machinery, Skp subsequently serves as a sacrificial adaptor protein to directly facilitate the degradation of defective OMP substrates by the periplasmic protease DegP. We conclude that Skp acts to ensure efficient β-barrel folding by directly mediating the displacement and degradation of assembly-compromised OMP substrates from the Bam complex.**

outer membrane protein biogenesis | periplasmic chaperones | Bam complex | β-barrel

The cell envelopes of gram-negative bacteria, mitochondria, and chloroplasts all contain an outer membrane (OM) consisting of integral transmembrane proteins that assume a β-barrel conformation (1, 2). In gram-negative bacteria such as *Escherichia coli*, β-barrel outer membrane proteins (OMPs) contribute to the selective permeability of the OM, protecting the cell from harmful molecules while still allowing for the uptake of nutrients (3). Structurally and functionally diverse OMPs serve a number of roles critical to cell viability, namely the selective passage of small molecules, efflux of toxins, insertion of lipopolysaccharide (LPS) onto the cell surface, and assembly of OMPs themselves (1, 4). Reflective of their importance in maintaining cellular integrity, defects in OMP biogenesis confer sensitivity to a wide array of toxic molecules including detergents, bile salts, and most importantly, antibiotics (5, 6). As such, considerable efforts have been made to identify agents that inhibit essential cellular processes performed by OMPs (7–12), with hopes of hastening the development of novel therapeutics to combat the ever-growing threat of antibiotic-resistant infections caused by gram-negative microbes (13, 14).

Ensuring efficient OMP biogenesis is a particularly challenging cellular feat. Newly synthesized OMPs must traverse the aqueous, oxidizing periplasm in an unfolded state, avoid self-aggregation, and subsequently complete proper assembly, all in an environment devoid of cellular energy such as adenosine triphosphate (15). A multitude of molecular chaperones and proteases function to overcome this challenge by minimizing unfolded OMP accumulation and facilitating OMP transport to the OM assembly machinery (16). Although more than a dozen chaperones and proteases with clear implications in OMP biogenesis have been identified (16–18), the most well-characterized and predominant proteins in *E. coli* are the chaperones SurA and Skp, as well as the chaperone protease DegP. Numerous genetic, biochemical, and proteomic studies have demonstrated that SurA is the primary periplasmic chaperone that facilitates transport of the bulk mass of OMP substrates to the OM (19–24). Skp and DegP, on the other hand, comprise a secondary, partially redundant OMP biogenesis pathway that primarily serves to minimize accumulation of unfolded OMPs, either by rescuing their assembly or promoting their degradation (19, 20).

Notably, Skp binds unfolded OMPs with dissociation constants in the low nanomolar range (25, 26), exceeding the binding affinities of either SurA or DegP (27–29), to form highly stable Skp–OMP complexes that display lifetimes on the order of hours (30). Given the substantial stability of Skp–OMP complexes, the precise mechanism of OMP release from Skp remains poorly understood. The rapid conformational dynamics of OMPs bound within the Skp cavity have been proposed to enable local substrate release that is ultimately driven by the recognition and folding of OMPs by the OM assembly machinery (30), thus coupling client release from Skp to the thermodynamic stability provided by OMP integration into a membrane (31). Indeed, substrate release and folding of OMPs from Skp–OMP complexes is enabled in vitro by incubation with OM folding machinery–containing liposomes (28, 32),

## Significance

**The outer membrane (OM) of gram-negative bacteria acts as a robust permeability barrier to enable cell survival in a wide variety of harsh environments. Crucial to OM integrity are β-barrel outer membrane proteins (OMPs) that are assembled into the membrane by the broadly conserved β-barrel assembly machine (Bam) complex. Here, we identify specific roles for the periplasmic chaperone Skp in functioning as a sacrificial adaptor protein to remove stalled substrates from the Bam complex, imposing an active quality control mechanism that ensures efficient assembly of nascent OMPs into the OM. This work identifies the molecular mechanism of the Skp/DegP functional relationship and clarifies the long-standing paradox of how substrate release from the high-affinity, long-lived Skp–OMP complex is achieved in vivo.**

Author contributions: A.N.C. and T.J.S. designed research; A.N.C. performed research; A.N.C. and T.J.S. analyzed data; and A.N.C. and T.J.S. wrote the paper.

The authors declare no competing interest.

This article is a PNAS Direct Submission.



[1]To whom correspondence may be addressed. Email: tsilhavy@princeton.edu.

This article contains supporting information online at http://www.pnas.org/lookup/suppl/doi:10.1073/pnas.2114997119/-/DCSupplemental.

Published December 28, 2021.

MICROBIOLOGY

demonstrating that Skp can facilitate productive OMP assembly. This mechanism of folding-driven substrate release has been similarly observed in genetic and biochemical studies indicating that Skp is capable of directly inserting OMPs into lipid bilayers in vitro (33), as well as the inner membrane in vivo (34), without assistance from the OM assembly machinery.

Whether OMPs are capable of being removed from Skp within physiological timescales in the absence of coupled folding, however, is not entirely clear. Under conditions of periplasmic stress, in which the burden of unfolded OMPs exceeds the rate at which they can be assembled, the activities of both Skp and DegP become crucial (19, 20, 24, 35). Given that Skp not only binds substrates with a higher affinity than DegP (29) but also does so several orders of magnitude faster (36), how unfolded OMPs are transferred from Skp to DegP for degradation under stress conditions is not obvious. Indeed, direct transfer of an OMP from Skp to DegP has yet to be demonstrated, and intriguingly, the formation of Skp–DegP–OMP ternary complexes has been reported in such experiments (29, 36).

Folding and insertion of nascent OMPs into the OM is catalyzed by the heteropentameric β-barrel assembly machine (Bam) complex, consisting of the BamA β-barrel and four accessory lipoproteins, BamBCDE (37, 38). Recent biochemical and structural studies have provided a relatively clear current model for the mechanism of β-barrel assembly. Following substrate recruitment to BamD (39), BamA catalyzes the sequential addition of β-hairpins in a C-to-N-terminal manner (40), with early folding occurring within the interior of the BamA barrel (41). Folding proceeds until membrane integration occurs, and subsequent stepwise hydrogen-bond formation between N and C substrate termini facilitates barrel closure and substrate release into the membrane (40).

One outstanding question concerns the fate of OMP substrates that have stalled while folding on the Bam complex. Protein misfolding in the periplasm, translational error, or impaired Bam complex function can result in substrates arresting on the assembly machinery, a condition that can ultimately be lethal if left unchecked (42–44). Until recently, investigations of stalled OMP substrates have been largely impeded by a lack of structurally defined folding intermediates and the absence of an established general mechanism of OMP assembly. Several studies to date have utilized mutant alleles of the large β-barrel LptD to probe Bam complex assembly (39, 41, 45, 46), and multiple proteases that degrade assembly-compromised LptD within distinct stages of its folding regime have been identified (46, 47). It is unclear, however, whether these stringent quality control mechanisms monitoring assembly of LptD are exerted on all β-barrel substrates or whether LptD represents a unique case given its remarkably complex folding trajectory (48). Given that OMP assembly by the Bam complex has evolved to be incredibly efficient—so efficient that unfolded OMPs cannot be detected at steady state—it stands to reason that quality control mechanisms ensuring the efficient assembly of all β-barrel substrates exist. Recently, it has been shown that extracellular loop deletions within the C-terminal half of the BamA β-barrel cause early folding defects and thus render stalled BamA susceptible to proteolysis by DegP (40). How DegP actively disengages a partially folded, stalled substrate from its folding on BamA, given the relatively weak and slow nature of DegP binding, is not obvious.

Here, we have utilized an assembly-defective variant of a slow-folding β-barrel OMP to investigate the fate of substrates that engage the OM assembly machinery but otherwise fail to undergo efficient folding and membrane integration. We identify a specific role for the periplasmic chaperone Skp in facilitating the degradation of defective OMP substrates by the protease DegP, thus imposing an active quality control mechanism that serves to remove assembly-compromised substrates from the Bam complex. Strikingly, we find that Skp is degraded alongside its bound substrate by DegP, thereby functioning as a sacrificial adaptor protein. By evaluating the requirement for Skp in degradation of a series of sequentially stalled β-barrel substrates, we find that Skp is only required to degrade substrates that have initiated folding on the Bam complex. Thus, β-barrel OMPs that have stalled during assembly specifically require Skp for their removal from the Bam complex and subsequent degradation by DegP. We conclude that Skp acts to ensure efficient β-barrel assembly by facilitating both the direct removal and degradation of stalled substrates from the Bam complex.

## Results

**Deletion of *skp* Suppresses the Assembly Defects of LptD$^{Y721D}$.** To gain insight into potential specialized roles of periplasmic chaperones during OMP biogenesis, we deliberately perturbed the OMP folding process by utilizing an assembly-defective mutant of an essential, slow-folding β-barrel substrate, LptD. LptD, together with its cognate lipoprotein LptE, forms the OM translocon of the Lpt (LPS transport) complex that facilitates the transport and insertion of LPS into the outer leaflet of the OM (49, 50). Folding of LptD is remarkably slow, orders of magnitude slower than other β-barrel substrates (51), taking roughly 20 min to fully complete (48). A mutant LptD substrate that harbors an amino acid substitution of a conserved tyrosine residue at position 721 for aspartate, LptD$^{Y721D}$, roughly triples the relatively long folding time of LptD by causing early assembly defects that are subsequent to substrate engagement (39). LptD$^{Y721D}$ is not deficient in its ability to be recruited to the Bam complex, but rather is slow to complete folding on BamA and is thereby subject to proteolytic degradation (39, 46). Consequently, the early assembly defects of LptD$^{Y721D}$ confer a recessive sensitivity to antibiotics due to reduced levels of functional LptDE translocons (39).

Degradation of LptD$^{Y721D}$ is known to be mediated by a number of periplasmic and OM proteases, most notably the periplasmic protease DegP (39, 46). However, deletion of *degP* primarily affects total levels of LptD$^{Y721D}$ without significant increases in the amount of fully folded, mature protein (46), suggesting that LptD$^{Y721D}$ assembly is somehow largely prevented even in the absence of substantial proteolysis. Indeed, deletion of *degP* is insufficient to rescue the permeability defects conferred by LptD$^{Y721D}$ in the presence of either bacitracin or vancomycin (46). Therefore, we reasoned that an additional periplasmic factor was responsible for preventing efficient LptD$^{Y721D}$ assembly even in the absence of LptD$^{Y721D}$ proteolysis.

Strikingly, we found that deletion of *skp* significantly suppressed the assembly defects of LptD$^{Y721D}$, as indicated by a restoration of resistance to both bacitracin and vancomycin (Fig. 1*A*). Additionally, while deletion of *degP* in an *lptD$_{Y721D}$* genetic background decreased viability in the absence of antibiotic (Fig. 1*A*), as previously observed (46), further deletion of *skp* rescued cellular viability (Fig. 1*A*). These results imply that even in the absence of substantial proteolysis by DegP, LptD$^{Y721D}$ assembly is largely prevented by Skp. Moreover, in the absence of Skp, efficient degradation of LptD$^{Y721D}$ by DegP must not occur.

To directly assess the effects of *skp* deletion on LptD$^{Y721D}$ assembly, we examined the oxidation state of LptD$^{Y721D}$ in the presence or absence of *skp* and/or *degP*. Upon completion of barrel folding, LptD undergoes a complex oxidative rearrangement to form two intramolecular disulfide bonds between nonconsecutive pairs of cysteine residues (48). Because only mature, properly assembled LptD adopts two nonconsecutive disulfide bonds (52), oxidation state thus serves as a reliable proxy for LptD assembly. Examination of LptD$^{Y721D}$ assembly

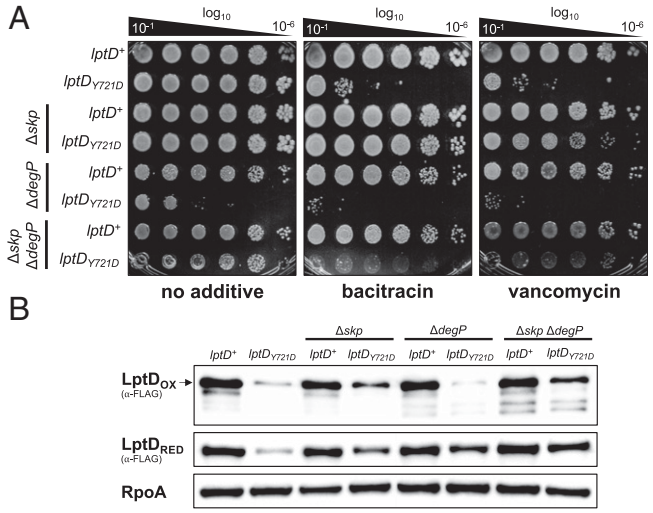


**Fig. 1.** Deletion of *skp* suppresses the assembly defects of LptD$^{Y721D}$. (*A*) Deletion of *skp* suppresses the OM defects conferred by LptD$^{Y721D}$. The indicated strains were grown overnight at 30 °C in LB medium, 10-fold serially diluted, and replica plated onto Mueller Hinton II agar supplemented with either 575 mg/L bacitracin or 90 mg/L vancomycin as indicated. Plates were incubated overnight at 37 °C. Results are representative of at least three independent experiments. (*B*) Deletion of *skp* improves LptD$^{Y721D}$ assembly. The indicated strains were grown overnight at 37 °C, and assembly of LptD$^{Y721D}$ was assayed by nonreducing (LptD$_{OX}$) or reducing (LptD$_{RED}$) SDS-PAGE followed by immunoblotting. RpoA levels are shown as a loading control. Blots are representative of at least three independent experiments.

using both nonreducing and reducing sodium dodecyl sulfate polyacrylamide gel electrophoresis (SDS-PAGE) revealed that while deletion of either *skp* or *degP* increased the relative levels of total reduced LptD$^{Y721D}$ (Fig. 1*B*), only deletion of *skp* promoted the assembly of properly oxidized, mature LptD$^{Y721D}$ (Fig. 1*B*). These findings demonstrate that the beneficial effects observed upon deletion of *skp* are a direct result of improved LptD$^{Y721D}$ assembly.

Taken together, these results suggest that LptD$^{Y721D}$ is only able to reside on the Bam complex long enough to complete its lengthy assembly process if Skp specifically is absent. Given that LptD$^{Y721D}$ is recruited normally to the OM assembly machinery (39), we conclude that Skp functions to remove assembly-defective LptD$^{Y721D}$ from the Bam complex in order to directly or indirectly facilitate its degradation by DegP.

**Skp Is Degraded with Bound Substrate by DegP.** Given that Skp was largely responsible for preventing efficient LptD$^{Y721D}$ assembly, we next wondered whether Skp was directly facilitating the degradation of assembly-defective substrates such as LptD$^{Y721D}$ by DegP. To address this hypothesis, we first utilized in vivo protein stability assays to monitor the degradation kinetics of LptD$^{Y721D}$ in the absence of translation. Diploid strains expressing 3×FLAG-tagged LptD or LptD$^{Y721D}$ from a low-copy plasmid were used in order to complement the recessive OM defects conferred by LptD$^{Y721D}$ (39). In cells harboring wild-type LptD, total levels of LptD remained relatively constant following addition of excess spectinomycin (Fig. 2 *A* and *B*). However, in cells expressing LptD$^{Y721D}$, significant degradation of LptD$^{Y721D}$ was observed over a period of 45 min following inhibition of protein synthesis. Importantly, the degradation of LptD$^{Y721D}$ could be prevented upon deletion of either *skp* or *degP* (Fig. 2 *A* and *B*), suggesting that both Skp and DegP are required for efficient degradation of LptD$^{Y721D}$.

Previously, our laboratory found that the periplasmic chaperone CpxP functions as a DegP adaptor protein to suppress the toxicity conferred by misfolded pilin subunits in the periplasm (53). Notably, CpxP's enhancement of DegP-mediated proteolysis requires degradation of both the adaptor protein CpxP and its bound substrate by DegP (53). Given the requirement for Skp in efficient degradation of LptD$^{Y721D}$ (Fig. 2 *A* and *B*) and the substantial affinity of Skp–OMP binding (25, 26, 29), we wondered whether Skp was similarly functioning as a sacrificial adaptor protein to directly mediate LptD$^{Y721D}$ proteolysis by DegP. To evaluate this possibility, we monitored the degradation kinetics of Skp using the same in vivo protein stability assay conditions described above. Indeed, while Skp levels remained relatively constant in a wild-type strain, Skp was rapidly degraded in an LptD$^{Y721D}$-dependent manner (Fig. 2 *C* and *D*). Moreover, degradation of Skp could be prevented upon deletion of *degP* (Fig. 2 *C* and *D*), demonstrating that DegP was mediating the observed Skp proteolysis. Taken together, we conclude that the periplasmic chaperone Skp functions as a sacrificial adaptor protein that is degraded with bound LptD$^{Y721D}$ by the periplasmic protease DegP.

**Skp Functions to Remove Stalled OMPs from the Bam Complex.** Since the folding defects of LptD$^{Y721D}$ are subsequent to engagement with the OM assembly machinery (39), we next wondered whether Skp functions generally to disengage OMPs that have stalled during folding on the Bam complex and are otherwise inaccessible for degradation by DegP. To test this hypothesis, we wished to design a series of OMP substrates that would stall at discrete points during the folding process and varied in the degree of assembly at the point of stalling. Folding of the BamA β-barrel by the Bam complex was recently shown to proceed in a C-to-N-terminal manner, with deletion of each extracellular loop within the BamA β-barrel causing substrates to stall at distinct points in assembly through slowed formation of β-hairpins (40). Extracellular loop deletions within the C-terminal half of the BamA β-barrel cause an early stalling in assembly and render BamA susceptible to degradation by DegP (40). We therefore reasoned that employing analogous C-terminal extracellular loop deletions for the model OMP LamB would allow us to evaluate the specific requirement for Skp in the degradation of stalled substrates by DegP. Moreover, because LamB exists functionally as a trimer, discrimination between the effects of *skp* deletion on both degradation and assembly of mutant substrates can be discerned by assaying levels of total monomeric and functional trimeric LamB, respectively.

A series of plasmid constructs harboring either full-length LamB or LamB that lacked one of nine extracellular loops (Fig. 3*A*) was generated and expressed in wild-type, Δ*skp*, Δ*degP*, and Δ*skp* Δ*degP* genetic backgrounds. Levels of both total monomeric and functional trimeric LamB were then assayed to determine the requirement for Skp in either stabilization or assembly of mutant LamB proteins, respectively. Similarly to the BamA β-barrel (40), deletions of extracellular loops within the C-terminal half of LamB (ΔL9–ΔL6) resulted in substantial LamB degradation in wild-type genetic backgrounds and showed significantly increased levels of total monomeric LamB upon *degP* deletion (Fig. 3*B*), indicating early folding defects. Defects were similarly apparent in the amount of functional LamB trimer, where all mutant LamB proteins showed significantly reduced levels of trimeric LamB compared to wild-type protein (Fig. 3*B*). For the C-terminal–most extracellular loop deletion (ΔL9), we observed increased levels of trimeric LamB upon deletion of *skp* or *degP* (Fig. 3*B*), suggesting that LamB$^{\Delta L9}$ is stalled at a point during folding at which Skp is not absolutely required for its degradation. However, for all subsequent extracellular loop deletions (ΔL8–ΔL6), efficient assembly into trimeric LamB specifically required that Skp be absent (Fig. 3*B*). Given that LamB$^{\Delta L8}$, LamB$^{\Delta L7}$, and LamB$^{\Delta L6}$ are

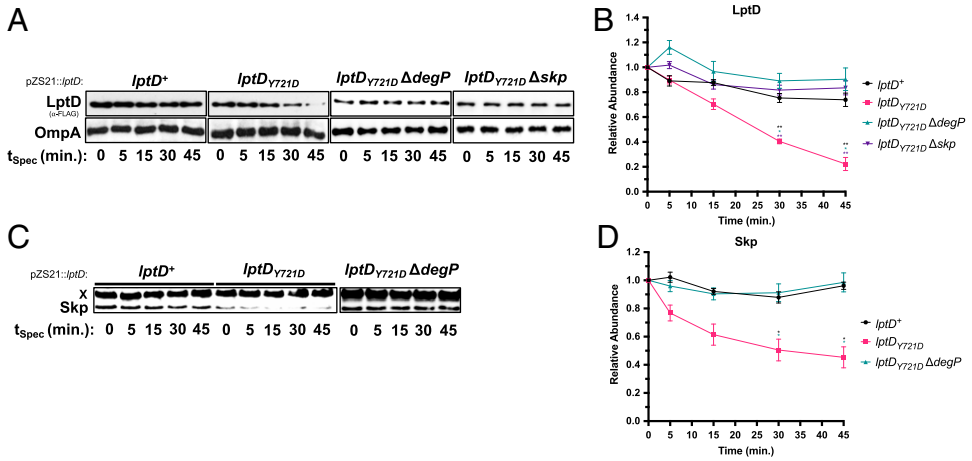


**Fig. 2.** Skp is degraded with substrate by DegP. (*A*) LptD$^{Y721D}$ is degraded in a Skp- and DegP-dependent manner. In vivo protein stability assays were performed to monitor LptD$^{Y721D}$ degradation in the absence of translation. The indicated strains were grown to midlogarithmic phase at 37 °C and treated with 300 μg/mL spectinomycin to inhibit de novo protein synthesis. Aliquots of each culture were taken at the indicated timepoints and analyzed by SDS-PAGE and immunoblotting. OmpA immunoblots are shown as a loading control. Blots are representative of at least three independent experiments. (*B*) Quantification of immunoblotting data shown in *A* over three independent experiments. Plotted data represent protein abundance over time relative to the initial abundance at $t = 0$. Individual datapoints represent the mean ± SEM. Statistical significance was determined by two-way ANOVA with Tukey's post hoc test. $*P < 0.05$; $**P < 0.01$. (*C*) Skp is degraded in an LptD$^{Y721D}$- and DegP-dependent manner. In vivo protein stability assays were performed as described in *A* and analyzed by SDS-PAGE and immunoblotting. The upper band is a cross-reactive protein (X) that serves as a loading control. Blots are representative of at least three independent experiments. (*D*) Quantification of immunoblotting data shown in *C* over three independent experiments. Plotted data represent protein abundance over time relative to the initial abundance at $t = 0$. Individual datapoints represent the mean ± SEM. Statistical significance was determined by two-way ANOVA with Tukey's post hoc test. $*P < 0.05$.

expected to have templated either three, five, or seven β-strands prior to the point of stalling, respectively (Fig. 3*A*), these results suggest that Skp is specifically required to remove stalled substrates that have already initiated folding on the Bam complex.

To further test this model, we wished to confirm that a Skp-dependent substrate (e.g., LamB$^{\Delta L7}$), but not a Skp-independent substrate (e.g., LamB$^{\Delta L9}$), was undergoing proteolysis in a Skp-dependent manner. As before, we utilized in vivo protein stability assays to monitor the degradation kinetics of both LamB and Skp in strains expressing either LamB$^{\Delta L9}$ or LamB$^{\Delta L7}$. In evaluating LamB stability, we found that both LamB$^{\Delta L9}$ and LamB$^{\Delta L7}$ underwent significant degradation over the course of 45 min posttreatment with translational inhibitor, with LamB$^{\Delta L7}$ being degraded at a slightly slower overall rate than LamB$^{\Delta L9}$ (Fig. 4 *A* and *B*). However, upon examining the stability of Skp, we observed significant Skp degradation only for LamB$^{\Delta L7}$- and not LamB$^{\Delta L9}$-expressing strains (Fig. 4 *C* and *D*). These data suggest that the degradation of LamB$^{\Delta L7}$ by DegP requires prior removal of stalled LamB$^{\Delta L7}$ from the Bam complex by Skp.

Given the enormous stability of paired β-strands within a membrane environment, it seemed unlikely that the displacement activity of Skp would also extend to late-stage folding intermediates. To address this possibility, we first examined the effects of *skp* deletion on the late-stalled substrates LptD4213 (45, 54) and LamB$^{\Delta L5}$, both of which would be predicted to have templated a substantial number of β-strands prior to the point of stalling. Deletion of *skp* and/or *degP* had no discernible

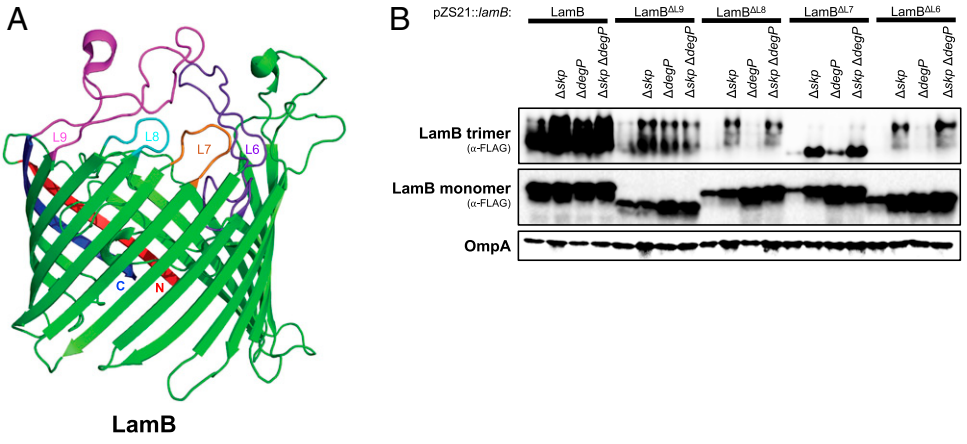


**Fig. 3.** Skp functions to remove stalled substrates from the Bam complex. (*A*) Structure of a LamB monomer depicting extracellular loops 6 through 9. The N- and C-terminal β-strands are shown in red and blue, respectively. Images were generated from the LamB crystal structure (Protein Data Bank ID: 1mal) using PyMOL. (*B*) Efficient assembly of LamB$^{\Delta L8}$, LamB$^{\Delta L7}$, and LamB$^{\Delta L6}$ specifically requires that Skp is absent. The indicated strains were grown overnight at 30 °C, and levels of trimeric LamB were assayed by seminative SDS-PAGE followed by immunoblotting. For simultaneous analysis of total monomeric LamB levels, an aliquot of each sample was boiled (denatured) and analyzed by SDS-PAGE and immunoblotting. OmpA levels are shown as a loading control. Blots are representative of at least three independent experiments.

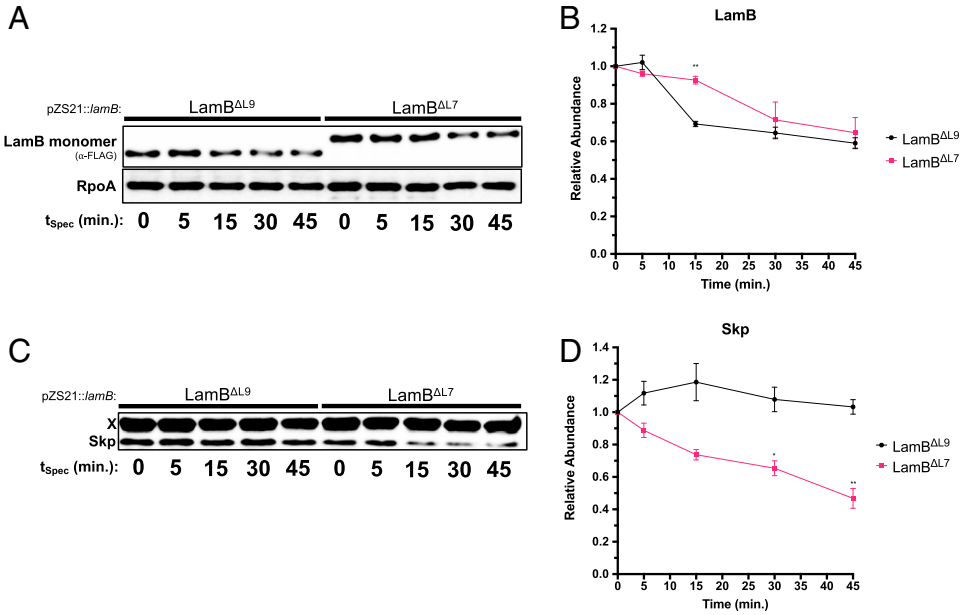


**Fig. 4.** Skp is only required to degrade substrates that have initiated folding on the Bam complex. (*A*) Both LamB$^{\Delta L9}$ and LamB$^{\Delta L7}$ undergo degradation over the course of 45 min following inhibition of protein synthesis. The indicated strains were grown to midlogarithmic phase at 37 °C and treated with 300 μg/mL spectinomycin to inhibit de novo protein synthesis. Aliquots of each culture were taken at the indicated timepoints and analyzed by SDS-PAGE and immunoblotting. RpoA levels are shown as a loading control. Blots are representative of at least three independent experiments. (*B*) Quantification of immunoblotting data shown in *A* over three independent experiments. Plotted data represent protein abundance over time relative to the initial abundance at $t = 0$. Individual datapoints represent the mean ± SEM. Statistical significance was determined by two-way ANOVA with Sidak's post hoc test. $^{**}P < 0.01$. (*C*) Skp is only degraded in LamB$^{\Delta L7}$-expressing strains. In vivo protein stability assays were performed as described in *A* and analyzed by SDS-PAGE and immunoblotting. The upper band is a cross-reactive protein (X) that serves as a loading control. Blots are representative of at least three independent experiments. (*D*) Quantification of immunoblotting data shown in *C* over three independent experiments. Plotted data represent protein abundance over time relative to the initial abundance at $t = 0$. Individual datapoints represent the mean ± SEM. Statistical significance was determined by two-way ANOVA with Sidak's post hoc test. $^{*}P < 0.05$; $^{**}P < 0.01$.

effect on LptD4213 assembly (*SI Appendix*, Fig. S1*A*), in agreement with previous observations that LptD4213 is not a substrate of DegP (46, 55). In contrast to prior LamB loop deletions (ΔL9–ΔL6), LamB$^{\Delta L5}$ was largely stable and not subject to substantial proteolysis in a wild-type genetic background (*SI Appendix*, Fig. S1*B*), similar to what was previously observed for late-stalled BamA substrates (40). Additionally, deletion of *skp* and/or *degP* did not significantly alter LamB$^{\Delta L5}$ trimerization (*SI Appendix*, Fig. S1*B*), suggesting that LamB$^{\Delta L5}$ is largely inaccessible to removal by Skp.

We then wished to determine whether Skp activity was directly correlated with the ability of a substrate to be extracted from the membrane following treatment with urea. It has previously been shown that early-stage β-barrel folding intermediates are susceptible to membrane extraction by either sodium carbonate or urea, whereas late-stage folding intermediates are not (39, 40, 55). During initial experiments performed with cells grown at 37 °C, we observed significant down-regulation of LamB ΔL9–ΔL6 expression when *degP* was deleted. This was likely due to $\sigma^E$-mediated translational repression via the small noncoding RNAs (sRNAs) MicA and RybB, of which LamB is a known regulatory target (56). To control for these effects, we performed two sets of experiments in parallel. First, membrane extractions were performed using the native LamB constructs with cells grown at 30 °C. At the same time, we ran identical extraction experiments with cells grown at 37 °C using LamB constructs in which the LamB signal sequences were replaced with the BamA signal sequence (BamA$_{(SS)}$-LamB) in order to circumvent sRNA-mediated translational repression, as BamA expression is not down-regulated by either MicA or RybB (56). Following translocation across the inner membrane and cleavage of either the LamB or BamA signal sequence, the mature LamB proteins produced are identical and thus would be expected to undergo identical assembly processes upon being delivered to the OM.

Notably, both sets of membrane extraction experiments—with either native LamB constructs expressed at 30 °C or BamA$_{(SS)}$-LamB constructs expressed at 37 °C—produced similar trends in substrate susceptibility to extraction by urea. Importantly, we observed a clear directionality in the substrate extraction profiles, with the C-terminal–most LamB loop deletions (LamB$^{\Delta L9}$, LamB$^{\Delta L8}$, and LamB$^{\Delta L7}$) being sensitive to urea extraction (Fig. 5 *A–D*), whereas the more N-proximal loop deletions (LamB$^{\Delta L6}$ and LamB$^{\Delta L5}$) were largely resistant to extraction (Fig. 5 *A–D*), suggesting that LamB indeed undergoes C-to-N-terminal folding in a manner similar to BamA (40). Strikingly, LamB$^{\Delta L6}$ was a substrate we observed to be markedly Skp-dependent in assembly (Fig. 3*B*), demonstrating that Skp is even capable of displacing a substrate that has completed sufficient folding to resist extraction by urea (Fig. 5 *A–D*).

Lastly, we conducted similar experiments to determine whether the inability of Skp to affect LptD4213 assembly was correlated with the membrane extraction susceptibility of LptD4213. We utilized LptD$^{Y721D}$ as a positive reference control, as LptD$^{Y721D}$ has been previously shown to be susceptible to membrane extraction with sodium carbonate (39). As predicted, LptD4213 was largely resistant to membrane extraction with urea, in stark contrast with the pronounced extraction susceptibility of LptD$^{Y721D}$ (Fig. 5 *E* and *F*). We conclude that Skp activity is correlated with the degree of substrate assembly, where substrates that proceed far enough in the assembly process (e.g., LamB$^{\Delta L5}$ and LptD4213) are inaccessible to displacement by Skp.

Taken together, we conclude that Skp functions to ensure efficient OMP assembly by specifically removing stalled

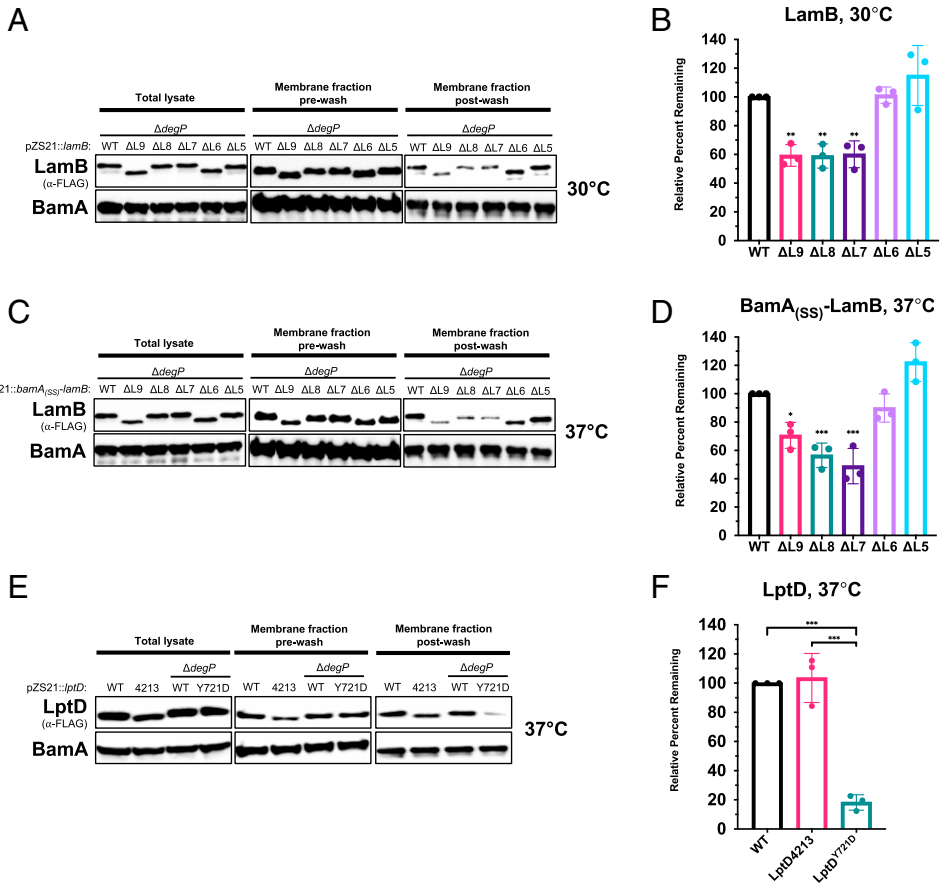


**Fig. 5.** Skp activity is correlated with the degree of substrate assembly. (*A*) Urea extraction experiments were performed for LamB substrates ΔL9 through ΔL5 using cells grown at 30 °C. Total lysate, membrane prewash, and membrane postwash fractions were analyzed by SDS-PAGE and immunoblotting. BamA immunoblots are shown as a loading control. Blots are representative of three independent experiments. (*B*) Quantification of immunoblotting data shown in *A* over three independent experiments. Pre- and postwash abundances were calculated relative to the amount of wild-type (WT) substrate present and the percent of substrate remaining was determined by dividing the postwash abundance by the prewash abundance. Plotted data represent the mean ± SD. Statistical significance was determined by one-way ANOVA with Dunnett's post hoc test. $^{**}P < 0.01$. (*C*) Urea extraction experiments were performed for $BamA_{SS}$-LamB substrates ΔL9 through ΔL5 using cells grown at 37 °C. Total lysate, membrane prewash, and membrane postwash fractions were analyzed by SDS-PAGE and immunoblotting. BamA immunoblots are shown as a loading control. Blots are representative of three independent experiments. (*D*) Quantification of immunoblotting data shown in *C* over three independent experiments. The percent of substrate remaining was calculated as described in *B*. Plotted data represent the mean ± SD. Statistical significance was determined by one-way ANOVA with Dunnett's post hoc test. $^{*}P < 0.05$; $^{***}P < 0.001$. (*E*) Urea extraction experiments were performed for LptD4213 and $LptD^{Y721D}$ using cells grown at 37 °C. Total lysate, membrane prewash, and membrane postwash fractions were analyzed by SDS-PAGE and immunoblotting. BamA immunoblots are shown as a loading control. Blots are representative of three independent experiments. (*F*) Quantification of immunoblotting data shown in *E* over three independent experiments. The percent of substrate remaining was calculated as described in *B*. LptD4213 and $LptD^{Y721D}$ abundances were calculated relative to the matched WT and Δ*degP* control strains, respectively. Plotted data represent the mean ± SD. Statistical significance was determined by one-way ANOVA with Tukey's post hoc test. $^{***}P < 0.001$.

substrates from the Bam complex and subsequently serving as a sacrificial adaptor protein for their degradation.

## Discussion

In this study, we have used the slow-folding β-barrel $LptD^{Y721D}$ as a tool to glean mechanistic insight into the fate of substrates that engage the OM assembly machinery but cannot efficiently membrane integrate. Our results reveal an active quality control mechanism in which Skp directly facilitates the degradation of assembly-compromised OMP substrates from the Bam complex. We have demonstrated that following sequestration of defective OMPs, Skp is degraded alongside its bound substrate by DegP, thereby functioning as a sacrificial adaptor protein to enhance DegP-mediated proteolysis. We have established that the specific requirement for Skp in DegP-mediated proteolysis is largely restricted to substrates that have initiated folding but have not yet membrane integrated (Fig. 6). Given that the catalytic mechanism of OMP assembly by the Bam complex consists of C-to-N-terminal, stepwise templating of β-hairpins (40), substrates lacking an extracellular loop must engage the assembly machinery prior to being recognized as defective. Thus, these results demonstrate that Skp is specifically required to displace and degrade assembly-compromised substrates from the Bam complex.

The high affinity (25) and remarkable stability (30) of Skp–OMP binding lends rationale as to why Skp must be degraded alongside its substrate by DegP. The rapid structural dynamics of the Skp–OMP complex comprise an equilibrium state that is both high in conformational entropy and low in enthalpy, enabling a conformational flexibility capable of permitting substrate release upon recognition of OMPs by downstream folding machinery (30). This substrate release from Skp is ultimately limited by differences in local affinity for any particular polypeptide segment, a criterion that is met by assembly machinery through recognition of the β-signal (30). Subsequent folding and insertion of substrates into the OM would enable

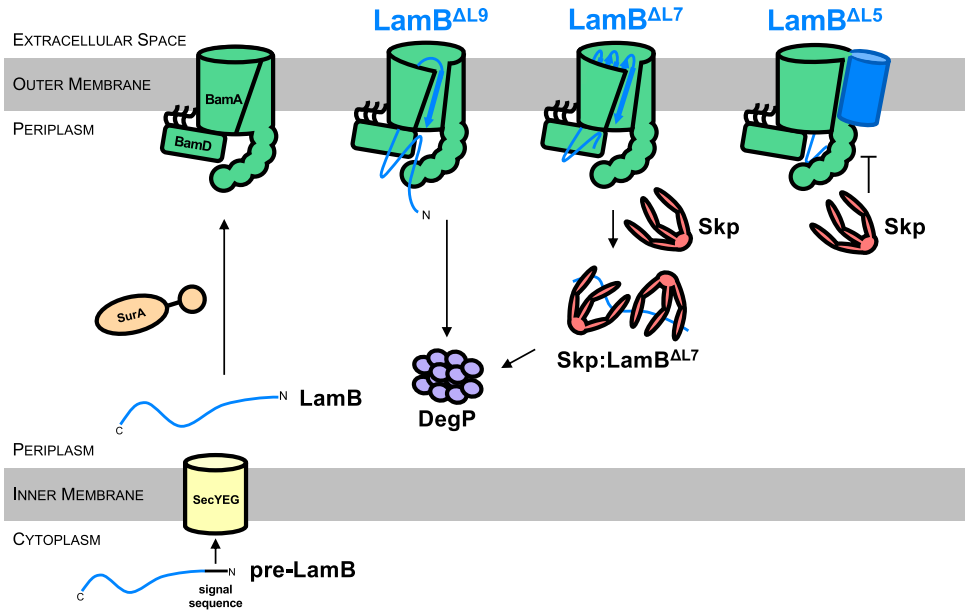


**Fig. 6.** Skp functions to remove stalled OMPs from the Bam complex and facilitates their degradation by DegP. Following translocation across the inner membrane and signal sequence cleavage, diffusion of nascent OMPs to the OM is predominantly mediated by SurA. Unfolded OMP substrates that accumulate in the periplasm or fail to initiate folding in a timely manner (e.g., LamB$^{\Delta L9}$) are directly accessible to degradation by DegP. In contrast, degradation of substrates that have stalled while folding (e.g., LamB$^{\Delta L7}$) requires prior removal from the Bam complex by Skp. Following OMP substrate displacement, Skp subsequently serves as a sacrificial adaptor protein to enhance DegP-mediated proteolysis and is degraded alongside its bound substrate. Upon completion of a substantial amount of folding (e.g., LamB$^{\Delta L5}$), OMP substrates are largely inaccessible to displacement by Skp, as substrate thermodynamic stability exceeds that of Skp–OMP binding.



rapid substrate release from Skp given the substantial thermodynamic stability afforded by OMP folding and integration into a membrane (31). In the absence of coupled folding, however, the relatively weak, slow nature of DegP–OMP binding (29, 36) is unable to facilitate sufficient substrate release from Skp in order to catalyze proteolysis in the absence of external energy. Consequently, the thermodynamic and kinetic limitations imposed by DegP-mediated degradation of a Skp-bound OMP require concerted proteolysis of both chaperone and substrate.

Notably, this observed proteolysis mechanism bears striking parallels to the concerted degradation of the periplasmic chaperone CpxP and misfolded pilin subunits by DegP (53). It is thus tempting to speculate that the requirement for adaptor proteins in DegP-mediated degradation might have evolved as a general mechanism to enable both rapid neutralization of particularly toxic substrates and their regulated proteolysis despite the kinetic and thermodynamic restraints of DegP binding. Indeed, mutations that stabilize the proteolytically active conformation of DegP and enhance the affinity of DegP binding confer dominant lethality under heat-shock conditions due to rogue protease activity (57), suggesting that additional regulatory mechanisms beyond simply controlling DegP proteolytic activity are necessary to viably combat periplasmic toxicity. The relatively rapid, high-affinity nature of Skp–OMP binding (25, 36) thereby ensures both timely neutralization of toxic substrates and enhancement of DegP protease activity in a manner that is regulated by the activity of Skp.

The high-affinity chaperone activity of Skp, which could represent a potential hazard to the cell if left uncontrolled, is carefully regulated by a disorder-to-order transition coupled to trimerization in response to substrate binding (58). In stark contrast, the activity of SurA is only weakly regulated, primarily through minor conformational rearrangements in response to substrate binding (59–61), effectively enabling largely constitutive chaperone activity. Importantly, these distinct differences in activation mechanism provide a potential means by which the chaperone activity of SurA could predominate over that of Skp under nonstress conditions despite its relatively weak binding to OMPs. Additionally, this work underscores the need for precise regulation of Skp chaperone activity, as rogue removal of OMPs that are in the process of folding on the Bam complex would almost certainly be deleterious. Rather, the activation mechanism of Skp (58) suggests that under conditions in which OMP assembly is compromised, prolonged dwelling of substrates on Bam likely promotes Skp monomer association, triggers subsequent trimerization, and allows for removal of stalled OMPs from assembly machinery, thus ensuring that the Skp-mediated displacement of OMPs from Bam is kinetically limited. Crucially, this mechanism of Skp-mediated disengagement of OMPs from assembly machinery implies that Skp—and not DegP, as previously suggested (44)—ultimately imposes the selective pressure for OMPs to rapidly membrane integrate, as substrates that fail to undergo membrane integration in a timely manner require removal from the Bam complex by Skp prior to their degradation by DegP. Moreover, the capability of Skp to mediate both displacement and subsequent degradation of folding-defective substrates explains the observed differential effects of *surA* and *skp* deletion on the assembly of OMPs harboring mutations in the β-signal (62).

Importantly, the ability to clear stalled substrates from the OM assembly machinery represents an additional role for Skp in OMP biogenesis and does not preclude its function as a chaperone under nonstress conditions. Rather, it suggests a more stringent mechanism of substrate release in which productive folding is likely necessary to remove OMPs from Skp in the absence of external energy. Only substrates that cannot complete proper folding are thereby subject to displacement from the Bam complex, thus imposing a quality control mechanism by which efficient OMP folding is ensured by the activity of Skp. Given that the direct interaction between Skp and DegP is relatively weak (29, 36)—likely to minimize premature degradation of Skp–OMP complexes—and that DegP binding is kinetically limited (36), it is possible that a single displaced OMP might undergo multiple attempts at productive folding

before being subjected to proteolysis, thus ensuring that only terminally defective OMP substrates are ultimately degraded.

The results presented here solidify the notion that Skp must interact in close proximity, and perhaps even directly, with the Bam complex, especially under conditions in which OMP assembly is compromised. Given that the folding of β-barrel substrates by the Bam complex is catalyzed by the interior surface of the BamA barrel (41), Skp must interact within close proximity of the BamA lumen in order to actively disengage assembly-compromised substrates. Although previous attempts to productively cross-link Skp to the Bam complex have been unsuccessful (20), this is not particularly surprising given the wealth of information establishing SurA as the primary periplasmic chaperone facilitating transport of the bulk mass of OMPs to the OM (19–24). Additionally, because Skp-mediated removal of OMPs from the Bam complex is likely kinetically limited, Skp may only transiently interact with the assembly machinery under nonstress conditions. Despite these limitations, it is possible that utilization of a Skp-dependent, slow-folding OMP substrate similar to those identified in this work may indeed enable productive cross-linking of Skp to the Bam complex.

It may seem paradoxical that the removal of a quality control system designed to disengage assembly-compromised substrates from the Bam complex does not impose significant consequences for cellular viability. However, tolerance to reduced Bam complex function is surprisingly robust under laboratory conditions, as evidenced by a roughly 90% reduction in BamA expression producing negligible effects on growth and viability (63, 64). For this reason, we think it is unlikely that any single slow-folding OMP substrate would compromise Bam complex function sufficiently to produce Skp-dependent growth defects under laboratory conditions. Intriguingly, Skp is required for full virulence in *Salmonella* and *Yersinia* murine infection models despite being completely dispensable for growth under laboratory conditions (65, 66), suggesting a crucial role for Skp in vivo. Given that *E. coli* Skp function is similarly dispensable for growth under laboratory conditions (20, 24), we speculate that Skp-mediated degradation of stalled OMP substrates may be critical in environments where the assembly of many β-barrel substrates is likely to be less efficient, including in vivo contexts.

Given that the OMP quality control mechanisms imposed by Skp are restricted to substrates that have not yet membrane integrated, one critical outstanding question is what, if anything, monitors OMP assembly beyond the point of membrane integration. Consistent with previous observations for BamA (40), late-stalled LamB substrates are largely stable (*SI Appendix*, Fig. S1*B*) and thus are likely not subject to proteolytic quality control. These observations lend the question of whether membrane integration represents a point of absolute commitment of assembly machinery to the folding of a particular substrate or whether additional quality control mechanisms capable of disengaging membrane-integrated substrates from the Bam complex exist. Additional studies investigating the quality control mechanisms that monitor late-stage folding by the Bam complex will be necessary to construct a complete understanding of the catalytic mechanism of β-barrel assembly.

## Materials and Methods

**Bacterial Strains and Growth Conditions.** All bacterial strains and plasmids used in this study are provided in the *SI Appendix*, Tables S1 and S2, respectively. Strains were constructed using standard microbiological techniques, as previously described (67). All plasmids were constructed using Gibson assembly or site-directed mutagenesis. Strains were grown in lysogeny broth (LB)supplemented with 20 mg/L chloramphenicol as appropriate. All strains were grown at either 30 or 37 °C as indicated. Deletion alleles originated from the Keio collection (68) and FLP recognition target–flanked kanamycin resistance cassettes were excised using the FLP recombinase as described previously (69). All LptD constructs contained a C-terminal 3×FLAG-tag (48), and all LamB constructs contained a 3×FLAG-tag flanked by 3× glycine residues (GGGDYKDHDGDYKDHDIDYKDDDDKGGG) inserted into extracellular loop four between codons 155 and 156 (70, 71). *lptD-3×FLAG* and *lptD$_{Y721D}$-3×FLAG* alleles were inserted at the native *lptD* locus through recombineering using *Collinsella stercoris* phage RecT (CspRecT) as described (72).

**Efficiency of Plating Assay.** Strains expressing 3×FLAG-tagged LptD or LptD$^{Y721D}$ from the native *lptD* locus were grown overnight in LB medium at 30 °C, 10-fold serially diluted, and replica plated onto Mueller Hinton II agar supplemented with 575 mg/L bacitracin or 90 mg/L vancomycin as indicated. Plates were incubated overnight at 37 °C.

**SDS-PAGE and Immunoblotting.** SDS-PAGE was performed using 10% hand-cast polyacrylamide gels with Tris/glycine/SDS running buffer. For Skp blots, SDS-PAGE was performed using Novex 16% tricine precast gels (Invitrogen) and Tris/tricine/SDS running buffer. Proteins were transferred to nitrocellulose membranes (GE Healthcare). Immunoblotting was performed using rabbit polyclonal antisera that recognize OmpA (1:10,000 dilution), Skp (1:8,000 dilution), RpoA (1:50,000 dilution), and BamA (1:10,000 dilution) or a mouse monoclonal antibody recognizing FLAG (1:5,000 dilution; Sigma-Aldrich). Goat anti-rabbit IgG-peroxidase (1:10,000; Sigma-Aldrich) or goat anti-mouse IgG-peroxidase (1:3,000; Bio-Rad) secondary antibodies were used for all immunoblots.

**In Vivo Protein Stability Assays.** Strains expressing plasmid-borne variants of 3×FLAG-tagged LptD or LamB were grown overnight at 30 °C and subcultured 1:100 into 10 mL LB medium. The resulting cultures were grown at 37 °C until an optical density at 600 nm ($OD_{600}$) of about 0.5 to 0.7 was reached, at which point 300 μg/mL spectinomycin was added to each culture to inhibit de novo protein synthesis. 1 mL aliquots of each culture were taken at the indicated timepoints, collected via centrifugation (16,100 × *g*, 1 min, room temperature), and flash frozen in an ethanol–dry ice bath. Frozen cell pellets were resuspended in a volume (mL) corresponding to the initial $OD_{600}$ divided by 7 of 2× Laemmli sample buffer (Bio-Rad) supplemented with 10% (vol/vol) β-mercaptoethanol. Samples were boiled for 10 min, and insoluble debris was pelleted by centrifugation (16,100 × *g*, 2 min, room temperature). Samples were analyzed by SDS-PAGE and immunoblotting as described above.

**Analysis of Trimeric LamB Levels.** Strains expressing plasmid-borne variants of 3×FLAG-tagged LamB were grown overnight at 30 °C. Cells corresponding to an $OD_{600}$ equivalent of 1 ($5 \times 10^8$ cells) were collected by centrifugation (16,100 × *g*, 2 min, room temperature) and resuspended in 25 μL 1× BugBuster Protein Extraction Reagent (MilliporeSigma) supplemented with protease inhibitor mixture (1:100; Sigma-Aldrich), Benzonase nuclease (1:100; MilliporeSigma), and 1 M $MgCl_2$ (1:100). Samples were lysed for 20 min at room temperature with gentle agitation. Then, 25 μL of 2× Laemmli sample buffer (Bio-Rad) supplemented with 10% (vol/vol) β-mercaptoethanol was added to dilute samples 1:2. Samples were centrifuged to pellet debris (16,100 × *g*, 2 min, 4 °C) and analyzed via seminative SDS-PAGE followed by immunoblotting as described above. For simultaneous analysis of total monomeric LamB levels, an aliquot of each sample was boiled for 10 min, centrifuged (16,100 × *g*, 2 min, room temperature), and analyzed by SDS-PAGE and immunoblotting as described above.

**Analysis of LptD Oxidation State.** Strains were grown overnight at 30 or 37 °C as indicated. Cells corresponding to an $OD_{600}$ equivalent of 1 ($5 \times 10^8$ cells) were collected by centrifugation (16,100 × *g*, 2 min, room temperature) and resuspended in 80 μL 2× Laemmli sample buffer (Bio-Rad) that lacked β-mercaptoethanol. Samples were boiled for 10 min, and insoluble debris was pelleted by centrifugation (16,100 × *g*, 2 min, room temperature). For simultaneous analysis of total reduced LptD levels, an aliquot of each sample was supplemented with 10% (vol/vol) β-mercaptoethanol and boiled for 2 min. Samples were analyzed by SDS-PAGE and immunoblotting as described above.

**Membrane Extraction with Urea.** Membrane extraction experiments were performed essentially as described (40) with minor modifications, as detailed in the *SI Appendix*, *Extended Materials and Methods*.

**Data Availability.** All study data are included in the article and/or *SI Appendix*.

**ACKNOWLEDGMENTS.** We thank members of the T.J.S. laboratory and Natividad Ruiz (The Ohio State University) for helpful discussions and critical reading of the manuscript. We also thank Irina Mikheyeva for generating 3×FLAG-tagged LamB. This research was supported by the National Institute of General Medical Sciences of the NIH under Award No. 5R35GM118024 (to T.J.S.). The content is solely the responsibility of the authors and does not necessarily represent the official views of the NIH.

1. T. J. Silhavy, D. Kahne, S. Walker, The bacterial cell envelope. *Cold Spring Harb. Perspect. Biol.* **2**, a000414 (2010).
2. C. L. Hagan, T. J. Silhavy, D. Kahne, β-Barrel membrane protein assembly by the Bam complex. *Annu. Rev. Biochem.* **80**, 189–210 (2011).
3. H. Nikaido, Molecular basis of bacterial outer membrane permeability revisited. *Microbiol. Mol. Biol. Rev.* **67**, 593–656 (2003).
4. D. P. Ricci, T. J. Silhavy, The Bam machine: A molecular cooper. *Biochim. Biophys. Acta* **1818**, 1067–1084 (2012).
5. N. Ruiz, B. Falcone, D. Kahne, T. J. Silhavy, Chemical conditionality: A genetic strategy to probe organelle assembly. *Cell* **121**, 307–317 (2005).
6. D. Missiakas, J. M. Betton, S. Raina, New components of protein folding in extracytoplasmic compartments of *Escherichia coli* SurA, FkpA and Skp/OmpH. *Mol. Microbiol.* **21**, 871–884 (1996).
7. N. Srinivas *et al.*, Peptidomimetic antibiotics target outer-membrane biogenesis in *Pseudomonas aeruginosa*. *Science* **327**, 1010–1013 (2010).
8. K. M. Storek *et al.*, Monoclonal antibody targeting the β-barrel assembly machine of *Escherichia coli* is bactericidal. *Proc. Natl. Acad. Sci. U.S.A.* **115**, 3692–3697 (2018).
9. S. U. Vetterli *et al.*, Thanatin targets the intermembrane protein complex required for lipopolysaccharide transport in *Escherichia coli*. *Sci. Adv.* **4**, eaau2634 (2018).
10. E. M. Hart *et al.*, A small-molecule inhibitor of BamA impervious to efflux and the outer membrane permeability barrier. *Proc. Natl. Acad. Sci. U.S.A.* **116**, 21748–21757 (2019).
11. A. Luther *et al.*, Chimeric peptidomimetic antibiotics against gram-negative bacteria. *Nature* **576**, 452–458 (2019).
12. Y. Imai *et al.*, A new antibiotic selectively kills gram-negative pathogens. *Nature* **576**, 459–464 (2019).
13. E. D. Brown, G. D. Wright, Antibacterial drug discovery in the resistance era. *Nature* **529**, 336–343 (2016).
14. E. Tacconelli *et al.*; WHO Pathogens Priority List Working Group, Discovery, research, and development of new antibiotics: The WHO priority list of antibiotic-resistant bacteria and tuberculosis. *Lancet Infect. Dis.* **18**, 318–327 (2018).
15. A. Konovalova, D. E. Kahne, T. J. Silhavy, Outer membrane biogenesis. *Annu. Rev. Microbiol.* **71**, 539–556 (2017).
16. M. Merdanovic, T. Clausen, M. Kaiser, R. Huber, M. Ehrmann, Protein quality control in the bacterial periplasm. *Annu. Rev. Microbiol.* **65**, 149–168 (2011).
17. F. Stull, J.-M. Betton, J. C. A. Bardwell, Periplasmic chaperones and prolyl isomerases. *Ecosal Plus* **8**, ESP-0005-2018 (2018).
18. J. Weski, M. Ehrmann, Genetic analysis of 15 protein folding factors and proteases of the *Escherichia coli* cell envelope. *J. Bacteriol.* **194**, 3225–3233 (2012).
19. A. E. Rizzitello, J. R. Harper, T. J. Silhavy, Genetic evidence for parallel pathways of chaperone activity in the periplasm of *Escherichia coli*. *J. Bacteriol.* **183**, 6794–6800 (2001).
20. J. G. Sklar, T. Wu, D. Kahne, T. J. Silhavy, Defining the roles of the periplasmic chaperones SurA, Skp, and DegP in *Escherichia coli*. *Genes Dev.* **21**, 2473–2484 (2007).
21. S. W. Lazar, R. Kolter, SurA assists the folding of *Escherichia coli* outer membrane proteins. *J. Bacteriol.* **178**, 1770–1773 (1996).
22. P. E. Rouvière, C. A. Gross, SurA, a periplasmic protein with peptidyl-prolyl isomerase activity, participates in the assembly of outer membrane porins. *Genes Dev.* **10**, 3170–3182 (1996).
23. D. Vertommen, N. Ruiz, P. Leverrier, T. J. Silhavy, J.-F. Collet, Characterization of the role of the *Escherichia coli* periplasmic chaperone SurA using differential proteomics. *Proteomics* **9**, 2432–2443 (2009).
24. K. Denoncin, J. Schwalm, D. Vertommen, T. J. Silhavy, J.-F. Collet, Dissecting the *Escherichia coli* periplasmic chaperone network using differential proteomics. *Proteomics* **12**, 1391–1401 (2012).
25. J. Qu, C. Mayer, S. Behrens, O. Holst, J. H. Kleinschmidt, The trimeric periplasmic chaperone Skp of *Escherichia coli* forms 1:1 complexes with outer membrane proteins via hydrophobic and electrostatic interactions. *J. Mol. Biol.* **374**, 91–105 (2007).
26. S. Pan, C. Yang, X. S. Zhao, Affinity of Skp to OmpC revealed by single-molecule detection. *Sci. Rep.* **10**, 14871 (2020).
27. J. Thoma, B. M. Burmann, S. Hiller, D. J. Müller, Impact of holdase chaperones Skp and SurA on the folding of β-barrel outer-membrane proteins. *Nat. Struct. Mol. Biol.* **22**, 795–802 (2015).
28. B. Schiffrin *et al.*, Effects of periplasmic chaperones and membrane thickness on BamA-catalyzed outer-membrane protein folding. *J. Mol. Biol.* **429**, 3776–3792 (2017).
29. C. Yang, S. Peng, C. Chen, X. S. Zhao, Molecular mechanism of networking among DegP, Skp and SurA in periplasm for biogenesis of outer membrane proteins. *Biochem. J.* **477**, 2949–2965 (2020).
30. B. M. Burmann, C. Wang, S. Hiller, Conformation and dynamics of the periplasmic membrane-protein-chaperone complexes OmpX-Skp and tOmpA-Skp. *Nat. Struct. Mol. Biol.* **20**, 1265–1272 (2013).
31. C. P. Moon, N. R. Zaccai, P. J. Fleming, D. Gessmann, K. G. Fleming, Membrane protein thermodynamic stability may serve as the energy sink for sorting in the periplasm. *Proc. Natl. Acad. Sci. U.S.A.* **110**, 4285–4290 (2013).
32. G. J. Patel, J. H. Kleinschmidt, The lipid bilayer-inserted membrane protein BamA of *Escherichia coli* facilitates insertion and folding of outer membrane protein A from its complex with Skp. *Biochemistry* **52**, 3974–3986 (2013).
33. G. J. Patel, S. Behrens-Kneip, O. Holst, J. H. Kleinschmidt, The periplasmic chaperone Skp facilitates targeting, insertion, and folding of OmpA into lipid membranes with a negative membrane surface potential. *Biochemistry* **48**, 10235–10245 (2009).
34. M. Grabowicz, D. Koren, T. J. Silhavy, The CpxQ sRNA negatively regulates Skp to prevent mistargeting of β-barrel outer membrane proteins into the cytoplasmic membrane. *MBio* **7**, e00312–e00316 (2016).
35. A. Konovalova *et al.*, Inhibitor of intramembrane protease RseP blocks the $\sigma^E$ response causing lethal accumulation of unfolded outer membrane proteins. *Proc. Natl. Acad. Sci. U.S.A.* **115**, E6614–E6621 (2018).
36. S. Wu *et al.*, Interaction between bacterial outer membrane proteins and periplasmic quality control factors: A kinetic partitioning mechanism. *Biochem. J.* **438**, 505–511 (2011).
37. T. Wu *et al.*, Identification of a multicomponent complex required for outer membrane biogenesis in *Escherichia coli*. *Cell* **121**, 235–245 (2005).
38. J. G. Sklar *et al.*, Lipoprotein SmpA is a component of the YaeT complex that assembles outer membrane proteins in *Escherichia coli*. *Proc. Natl. Acad. Sci. U.S.A.* **104**, 6400–6405 (2007).
39. J. Lee *et al.*, Substrate binding to BamD triggers a conformational change in BamA to control membrane insertion. *Proc. Natl. Acad. Sci. U.S.A.* **115**, 2359–2364 (2018).
40. D. Tomasek *et al.*, Structure of a nascent membrane protein as it folds on the BAM complex. *Nature* **583**, 473–478 (2020).
41. J. Lee *et al.*, Formation of a β-barrel membrane protein is catalyzed by the interior surface of the assembly machine protein BamA. *eLife* **8**, e49787 (2019).
42. E. M. Hart, M. Gupta, M. Wühr, T. J. Silhavy, The synthetic phenotype of Δ*bamB* Δ*bamE* double mutants results from a lethal jamming of the Bam complex by the lipoprotein RcsF. *MBio* **10**, e00662-19 (2019).
43. M. Tata, A. Konovalova, Improper coordination of BamA and BamD results in Bam complex jamming by a lipoprotein substrate. *MBio* **10**, e00660-19 (2019).
44. J. H. Peterson, A. M. Plummer, K. G. Fleming, H. D. Bernstein, Selective pressure for rapid membrane integration constrains the sequence of bacterial outer membrane proteins. *Mol. Microbiol.* **106**, 777–792 (2017).
45. J. Lee *et al.*, Characterization of a stalled complex on the β-barrel assembly machine. *Proc. Natl. Acad. Sci. U.S.A.* **113**, 8717–8722 (2016).
46. G. R. Soltes, N. R. Martin, E. Park, H. A. Sutterlin, T. J. Silhavy, Distinctive roles for periplasmic proteases in the maintenance of essential outer membrane protein assembly. *J. Bacteriol.* **199**, e00418-17 (2017).
47. S. Narita, C. Masui, T. Suzuki, N. Dohmae, Y. Akiyama, Protease homolog BepA (YfgC) promotes assembly and degradation of β-barrel membrane proteins in *Escherichia coli*. *Proc. Natl. Acad. Sci. U.S.A.* **110**, E3612–E3621 (2013).
48. S.-S. Chng *et al.*, Disulfide rearrangement triggered by translocon assembly controls lipopolysaccharide export. *Science* **337**, 1665–1668 (2012).
49. T. Wu *et al.*, Identification of a protein complex that assembles lipopolysaccharide in the outer membrane of *Escherichia coli*. *Proc. Natl. Acad. Sci. U.S.A.* **103**, 11754–11759 (2006).
50. S.-S. Chng, N. Ruiz, G. Chimalakonda, T. J. Silhavy, D. Kahne, Characterization of the two-protein complex in *Escherichia coli* responsible for lipopolysaccharide assembly at the outer membrane. *Proc. Natl. Acad. Sci. U.S.A.* **107**, 5363–5368 (2010).
51. A. R. Ureta, R. G. Endres, N. S. Wingreen, T. J. Silhavy, Kinetic analysis of the assembly of the outer membrane protein LamB in *Escherichia coli* mutants each lacking a secretion or targeting factor in a different cellular compartment. *J. Bacteriol.* **189**, 446–454 (2007).
52. N. Ruiz, S.-S. Chng, A. Hiniker, D. Kahne, T. J. Silhavy, Nonconsecutive disulfide bond formation in an essential integral outer membrane protein. *Proc. Natl. Acad. Sci. U.S.A.* **107**, 12245–12250 (2010).
53. D. D. Isaac, J. S. Pinkner, S. J. Hultgren, T. J. Silhavy, The extracytoplasmic adaptor protein CpxP is degraded with substrate by DegP. *Proc. Natl. Acad. Sci. U.S.A.* **102**, 17775–17779 (2005).
54. B. A. Sampson, R. Misra, S. A. Benson, Identification and characterization of a new gene of *Escherichia coli* K-12 involved in outer membrane permeability. *Genetics* **122**, 491–501 (1989).
55. J. S. Wzorek, J. Lee, D. Tomasek, C. L. Hagan, D. E. Kahne, Membrane integration of an essential β-barrel protein prerequires burial of an extracellular loop. *Proc. Natl. Acad. Sci. U.S.A.* **114**, 2598–2603 (2017).
56. E. B. Gogol, V. A. Rhodius, K. Papenfort, J. Vogel, C. A. Gross, Small RNAs endow a transcriptional activator with essential repressor functions for single-tier control of a global stress regulon. *Proc. Natl. Acad. Sci. U.S.A.* **108**, 12875–12880 (2011).
57. S. Kim, R. T. Sauer, Distinct regulatory mechanisms balance DegP proteolysis to maintain cellular fitness during heat stress. *Genes Dev.* **28**, 902–911 (2014).
58. G. Mas *et al.*, Regulation of chaperone function by coupled folding and oligomerization. *Sci. Adv.* **6**, eabc5822 (2020).
59. D. P. Ricci, J. Schwalm, M. Gonzales-Cope, T. J. Silhavy, The activity and specificity of the outer membrane protein chaperone SurA are modulated by a proline isomerase domain. *MBio* **4**, e00540-13 (2013).
60. G. R. Soltes, J. Schwalm, D. P. Ricci, T. J. Silhavy, The activity of *Escherichia coli* chaperone SurA is regulated by conformational changes involving a parvulin domain. *J. Bacteriol.* **198**, 921–929 (2016).
61. A. N. Calabrese *et al.*, Inter-domain dynamics in the chaperone SurA and multi-site binding to its outer membrane protein clients. *Nat. Commun.* **11**, 2155 (2020).
62. X. Wang, J. H. Peterson, H. D. Bernstein, Bacterial outer membrane proteins are targeted to the Bam complex by two parallel mechanisms. *MBio* **12**, e00597-21 (2021).

63. S. K. Aoki *et al.*, Contact-dependent growth inhibition requires the essential outer membrane protein BamA (YaeT) as the receptor and the inner membrane transport protein AcrB. *Mol. Microbiol.* **70**, 323–340 (2008).
64. T. F. Mahoney, D. P. Ricci, T. J. Silhavy, Classifying β-barrel assembly substrates by manipulating essential Bam complex members. *J. Bacteriol.* **198**, 1984–1992 (2016).
65. G. Rowley *et al.*, The periplasmic chaperone Skp is required for successful *Salmonella* Typhimurium infection in a murine typhoid model. *Microbiology (Reading)* **157**, 848–858 (2011).
66. J. Weirich *et al.*, Identifying components required for OMP biogenesis as novel targets for antiinfective drugs. *Virulence* **8**, 1170–1188 (2017).
67. T. J. Silhavy, M. L. Berman, L. W. Enquist, *Experiments with Gene Fusions* (Cold Spring Harbor Laboratory, 1984).
68. T. Baba *et al.*, Construction of *Escherichia coli* K-12 in-frame, single-gene knockout mutants: The Keio collection. *Mol. Syst. Biol.*, **2**, 2006.0008 (2006).
69. K. A. Datsenko, B. L. Wanner, One-step inactivation of chromosomal genes in *Escherichia coli* K-12 using PCR products. *Proc. Natl. Acad. Sci. U.S.A.* **97**, 6640–6645 (2000).
70. S. Brown, Metal-recognition by repeating polypeptides. *Nat. Biotechnol.* **15**, 269–272 (1997).
71. T. S. Ursell, E. H. Trepagnier, K. C. Huang, J. A. Theriot, Analysis of surface protein expression reveals the growth pattern of the gram-negative outer membrane. *PLoS Comput. Biol.* **8**, e1002680 (2012).
72. T. M. Wannier *et al.*, Improved bacterial recombineering by parallelized protein discovery. *Proc. Natl. Acad. Sci. U.S.A.* **117**, 13689–13698 (2020).